

28. Malmgren, B., Kucera, M., Nyberg, J. & Waelbroeck, C. Comparison of available statistical and artificial neural network techniques for estimating past sea-surface temperatures from planktonic foraminifera census data. *Palaeoceanography* (in the press).
29. Bondevik, S., Birks, H. H., Gulliksen, S. & Mangerud, J. Late Weichselian marine ¹⁴C reservoir ages at the western coast of Norway. *Quat. Res.* **52**, 104–114 (1999).
30. Labeyrie, L. *et al.* Surface and deep hydrology of the northern Atlantic Ocean during the last 150,000 years. *Phil. Trans. R. Soc. Lond.* **348**, 255–264 (1995).

Supplementary information is available on Nature's World-Wide Web site (<http://www.nature.com>) or as paper copy from the London editorial office of Nature.

Acknowledgements

We thank E. Bard and G. Siani for discussions and comments. The data were acquired in collaboration with T. van Weering, J.-L. Turon, M. Labracherie and G. Auffret. We thank B. Lecoat and J. Tessier for processing the isotopic measurements. This study was supported by CNRS, CEA, INSU (PNEDC) and EU Environment Program.

Correspondence and requests for materials should be addressed to C.W. (e-mail: Claire.Waelbroeck@lscn.cnr.fr).

Direct observation of a submarine volcanic eruption from a sea-floor instrument caught in a lava flow

Christopher G. Fox*†, William W. Chadwick Jr†‡ & Robert W. Embley*

* NOAA/PMEL, Newport, Oregon 97365, USA
 ‡ 2115 SE OSU Drive, Oregon State University/NOAA, Newport, Oregon 97365, USA
 † These authors contributed equally to this work

Our understanding of submarine volcanic eruptions has improved substantially in the past decade owing to the recent ability to remotely detect such events¹ and to then respond rapidly with synoptic surveys and sampling at the eruption site. But these data are necessarily limited to observations after the event². In contrast, the 1998 eruption of Axial volcano on the Juan de Fuca ridge^{3,4} was monitored by *in situ* sea-floor instruments^{5–7}. One of these instruments, which measured bottom pressure as a proxy for vertical deformation of the sea floor, was overrun and entrapped by the 1998 lava flow. The instrument survived—being insulated from the molten lava by the solidified crust—and was later recovered. The data serendipitously recorded by this instrument reveal the duration, character and effusion rate of a sheet flow eruption on a mid-ocean ridge, and document over three metres of lava-flow inflation and subsequent drain-back. After the brief two-hour eruption, the instrument also measured gradual subsidence of 1.4 metres over the next several days, reflecting deflation of the entire volcano summit as magma moved into the adjacent rift zone. These findings are consistent with our understanding of submarine lava effusion, as previously inferred from seafloor observations, terrestrial analogues, and laboratory simulations^{8–11}.

Two Volcanic System Monitor (VSM) instruments were deployed at Axial volcano in October 1997, one near the centre of the caldera⁵ and one on the upper south rift zone, hereafter referred to as VSM1 and VSM2, respectively (Figs 1 and 2). The VSM instruments measure ambient pressure on the sea floor every 15 s with a Paroscientific digiquartz pressure sensor. The data processing methods are described in detail elsewhere^{5,12}, but include filtering to remove oceanographic phenomena and a correction for temperature. In August 1998, VSM2 was found to be trapped in the new lava flow (Fig. 1), but it was pulled free the following summer.

The rescued instrument was in surprisingly good condition. The

maximum temperature recorded inside VSM2 during the eruption was only 7.5 °C (Fig. 3)—remarkably low, considering that the instrument was sitting atop basaltic lava that was probably erupted at ~1,190 °C (M. Perfit, personal communication). This was apparently due to the thermal insulation provided by the surface crust that forms (and quickly thickens) when submarine lava flows come into contact with frigid sea water¹³.

The northern end of the 1998 lava flow where VSM2 was located (Fig. 2) is a long, narrow sheet flow⁴. Submarine sheet flows are thought to form by brief, relatively high-effusion-rate eruptions^{8,9}. Recent models^{10,11} suggest that such flows initially advance as thin lobate flows (20–30 cm thick), spreading at a rate that is rapid enough for the interior of the flow to remain a single fluid core beneath a solid upper crust. The flow spreads until it becomes laterally confined, and then 'inflates' upward. During inflation, the upper crust is uplifted (sometimes > 5 m) by hydraulic pressure within the flow interior—and lava pillars grow upward, connecting the upper and lower crusts¹⁰. Lava inflation continues until the eruption rate wanes or stops, at which point lava begins to drain back and the upper crust founders where it is left unsupported, leaving extensive areas of collapse within the flow.

Geologic mapping of the 1998 lava flow shows that VSM2 was located in the collapsed interior of the 1998 lava flow, ~3 m below nearby remnants of the uncollapsed upper crust and ~160 m west of the eruptive fissure (Fig. 2). The instrument had not been buried by lava, even though the lava level had been 3 m higher before collapse. This observation implies that lava initially flowed under the instrument, which became embedded in the upper crust of the flow when the flow subsequently inflated. During inflation, VSM2 was uplifted along with the upper crust (because of its table-like design) and then was set back down within the collapse area during the drain-back stage.

The dataset recovered from the VSM2 instrument directly recorded this sequence of events (Fig. 3). Uplift of the instrument began slowly at 14:55 on 25 January 1998 (all times GMT), after the onset of the earthquake swarm at 11:33 (ref. 3) and subsidence began at VSM1 at 14:51 (ref. 5). Rapid inflation abruptly started at 15:16 when VSM2 was uplifted 168 cm in the next 5 minutes, an average rate of 32 cm min⁻¹ (although instantaneous rates were as high as 73 cm min⁻¹). After a pause of 4 minutes, during which the instrument subsided 13 cm, inflation resumed for another 21 minutes which uplifted the instrument another 113 cm at a decreased rate of 5.5 cm min⁻¹. At 15:46, inflation dramatically slowed, probably owing to a sudden reduction in the effusion rate at the vent, and the instrument was only uplifted another 7 cm over the next 21 minutes. During this period the lava flow remained at or near its fully inflated thickness, and the recorded temperature reached its peak of 7.5 °C at 15:49 (Fig. 3).

At this point, lava inflation ended and lava drain-back began, presumably reflecting the end of lava effusion at the vent. Our

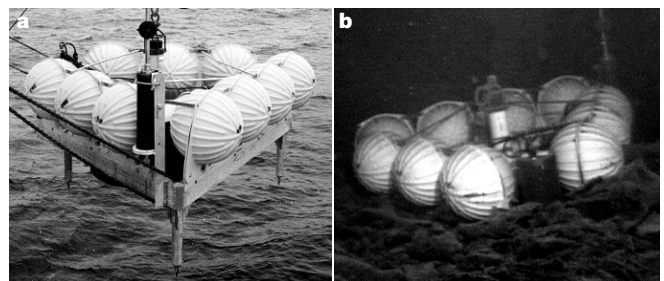


Figure 1 Views of the VSM2 instrument. **a**, At the surface during deployment (legs are 46 cm long), and **b**, on the sea floor, stuck in the 1998 lava flow at Axial volcano. Virtual animations and video clips of VSM2 (referred to as a 'rubbleometer') on the sea floor are available at <http://www.pmel.noaa.gov/vents/nemo/explorer/rumble.html>

interpretation is that the lava then drained directly back down into the vent, because the 1998 flow is relatively narrow here and because the slope direction within the collapse area is directly toward the eruptive fissure (Fig. 2). During lava drain-back, VSM2 subsided 281 cm, at a nearly uniform rate of 3.5 cm min⁻¹ (Fig. 3). The recorded temperature also declined during drain-back, reaching 5.2 °C at 17:16. When drain-back ended at 17:28, the instrument was only 24 cm higher than when it started, but over the next several hours it regained about 30 cm of lost elevation, perhaps during the waning stages of the eruption. A second peak in temperature (7.3 °C) was recorded at 18:12, following the end of drain-back, after which the temperature steadily declined. In the end, only 1 m of lava remained in the floor of the collapse area where the flow had previously inflated to a thickness of 3.5 m. The entire inflation/deflation cycle lasted only 2 hours and 33 minutes, but the duration of active lava effusion from the eruptive vent was probably only 72 minutes (the inflation phase).

The 1998 lava flow is ~350 m wide in the east–west direction at the latitude of the position of VSM2 (Fig. 2). The eruptive fissure is linear and roughly oriented north–south, as are the east and west edges of the lava flow. This simple flow geometry allows us to calculate volumetric rates of both eruption and drain-back in the vicinity of the VSM2 instrument, based on the pressure data. To make these estimates we assume that the lava flow is two-dimensional, exactly 300 m wide with vertical sides, and that the VSM2 data represent the lava level within the entire width of the flow. This approximation is reasonable as the flow is actually wider than 300 m, but tapers near its edges.

All the rates discussed below are expressed as a volumetric rate per 1-m length of eruptive fissure, as the eruption was from a line-source rather than a point-source. We have no way of estimating the initial effusion rate while lava spread out from the vent as a thin sheet before VSM2 began to record inflation. Once inflation began, a volumetric effusion rate of 2.7 m³ s⁻¹ is associated with the time period of the highest rate of lava inflation. The effusion rate then

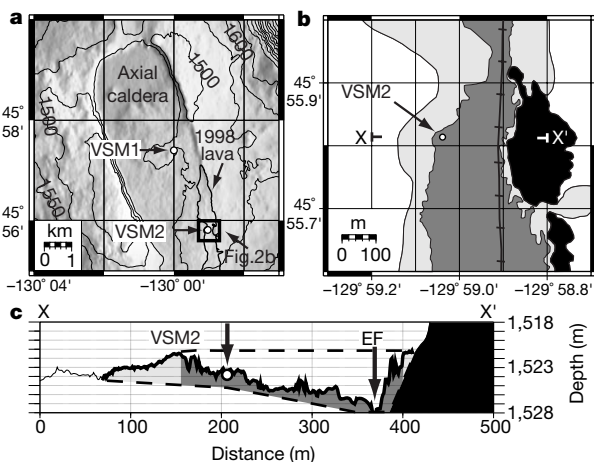


Figure 2 Location of the VSM2 instrument. **a**, Map of the caldera at Axial volcano, showing locations of the VSM1 and VSM2 instruments and the outline of the 1998 lava flow. Location of **b** is indicated. **b**, Detailed geologic map showing the location of VSM2 within the 1998 lava flow, based on scanning sonar bathymetry and bottom observations. Areas shown light grey and dark grey are respectively uncollapsed and collapsed parts of the 1998 flow; areas shown white and black are respectively older surrounding sheet flows and high-standing pillow flows. Hatched line is the 1998 eruptive fissure. X–X' is location of cross-section in **c**. **c**, Cross-section showing location of VSM2 within the collapsed interior of the 1998 lava flow, ~3 m below remnants of the flow's upper crust, and yet unburied by lava. Depth is shown as metres below the sea surface. EF, 1998 eruptive fissure. Dashed lines show probable upper and lower extent of 1998 lava flow before collapse. Shading as in **b**.

decreased by an order of magnitude to 0.27 m³ s⁻¹ during the slower second half of the inflation phase, and then dropped another order of magnitude to 0.016 m³ s⁻¹ during the interval when the flow was fully inflated. During drain-back, the rate that lava was flowing back into the vent was 0.17 m³ s⁻¹. This pattern of a brief burst at a high effusion rate followed by a longer period of waning rates is common at basaltic volcanoes¹⁴.

Laboratory analogue experiments have previously been used to associate the morphology of submarine lava flows with the effusion rates that may have produced them^{8,9}. The work we report here provides, we believe for the first time, a means to estimate directly the effusion rate for a submarine eruption—and we can compare these results with those predicted by the experimental models. The 1998 lava developed a lobate flow morphology as it spread out from the vent near VSM2. Geochemical analyses of the 1998 lava suggest that its viscosity at eruption was ~30 Pa s (M. Perfit, personal communication). If we assume that the effusion rate during this initial stage was the same as during the beginning of flow inflation (~3 m³ s⁻¹ per unit length of the vent), then Axial's 1998 flow would be consistent with the predictions from previous laboratory results^{8,9}, because it plots within the 'lobate' field, between the 'pillowed' and 'folded' domains (where the value of the dimensionless physical parameter, Ψ , is 3–13).

It is difficult to extrapolate these volumetric effusion rates per unit length of eruptive fissure to total eruption rates; this is because the VSM2 data only constrain the rates in the vicinity of the instrument, the eruptive fissure for the northern portion of the 1998 Axial eruption was probably ~2.6 km long, and the discharge rate and duration may have varied along its length. Nevertheless, if we assume the eruptive conditions were uniform along the entire eruptive fissure, the instantaneous total eruption rate would have

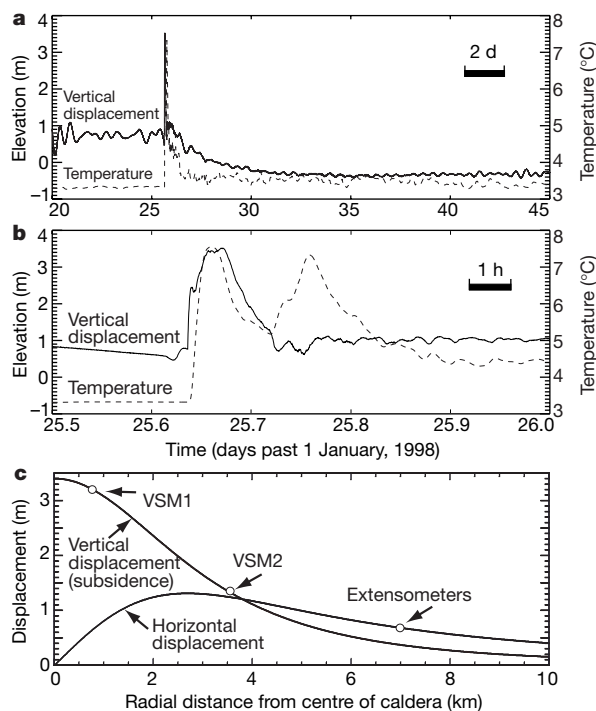


Figure 3 Data from the VSM2 instrument. **a**, Vertical displacement (solid line; from pressure data) and temperature (dashed line; measured inside a pressure case) from 20 January to 14 February 1998. **b**, Details of the vertical displacement and temperature records at the time of the eruption on 25 January. Zero elevation in **a** and **b** is arbitrary. **c**, Elastic point source deformation model¹⁹ showing how the VSM2 data fitted the curves previously derived from VSM1 and extensometer instruments⁶. Model assumes point-source is located 3.8 km beneath the centre of the caldera.

been as high as $7,000 \text{ m}^3 \text{ s}^{-1}$ early in the eruption, or $\sim 550 \text{ m}^3 \text{ s}^{-1}$ if averaged over the 72 minutes of flow inflation. These numbers are at the upper end of discharge rates reported for basaltic volcanoes on land^{14–18}.

After the inflation/drain-back signal in the VSM2 pressure record, the instrument also recorded a further gradual subsidence of the sea floor by 1.4 m over the next 5 days (Fig. 3). This part of the signal is due to the deflation of the summit of Axial volcano as magma moved from the reservoir beneath the caldera and into the south rift zone. This deflation signal was also observed by two other sea-floor instruments during the same time period: VSM1, deployed near the centre of the caldera, recorded a subsidence of 3.2 m (ref. 5), and an array of extensometers on Axial's north rift zone measured a 4-cm decrease of a 405-m-long horizontal baseline⁶. This distance decrease can be explained if the baseline endpoints moved 68 cm radially inward toward the centre of the caldera during deflation⁶. These are, to our knowledge, the first *in situ* ground deformation measurements made during a submarine volcanic eruption. The VSM1 and extensometer data were used—before the data were recovered from VSM2—to calculate⁶ the depth of the magma reservoir (3.8 km) and the volume of magma removed from the reservoir beneath the caldera ($207 \times 10^6 \text{ m}^3$), on the basis of a point-source elastic deformation model¹⁹. We note that the third data point from VSM2 fits exactly on the same subsidence curve predicted by this deformation model (Fig. 3c). This agreement gives increased confidence in the model results, which are also consistent with estimates of the depth of Axial's magma reservoir based on seismic tomography²⁰.

Little is known about deep-sea eruptions, because we have only been able to detect them for about a decade and none have ever been witnessed. The data we report here, recorded by the VSM2 instrument caught in the 1998 lava flow at Axial volcano, were obtained by fortuitous circumstance. The instrument was simply in the right place at the right time, with the right sensors, and happened to have the right physical design to survive the eruption. □

Received 17 April; accepted 28 June 2001.

1. Fox, C. G., Dziak, R. P., Matsumoto, H. & Schreiner, A. E. Potential for monitoring low-level seismicity on the Juan de Fuca Ridge using military hydrophone arrays. *Mar. Technol. Soc. J.* **27**, 22–30 (1994).
2. Perfit, M. R. & Chadwick, W. W. Jr in *Faulting and Magmatism at Mid-Ocean Ridges* (eds Buck, W. R., Delaney, P. T., Karson, J. A. & Lagabriele, Y. 59–116 (AGU Geophysical Monograph 106, American Geophysical Union, Washington DC, 1998).
3. Dziak, R. P. & Fox, C. G. The January 1998 earthquake swarm at Axial Volcano, Juan de Fuca Ridge: Hydroacoustic evidence of seafloor volcanic activity. *Geophys. Res. Lett.* **26**, 3429–3432 (1999).
4. Embley, R. W., Chadwick, W. W. Jr, Clague, D. & Stakes, D. The 1998 eruption of Axial Volcano: Multibeam anomalies and seafloor observations. *Geophys. Res. Lett.* **26**, 3425–3428 (1999).
5. Fox, C. G. In situ ground deformation measurements from the summit of Axial Volcano during the 1998 volcanic episode. *Geophys. Res. Lett.* **26**, 3437–3440 (1999).
6. Chadwick, W. W. Jr, Embley, R. W., Milburn, H. B., Meinig, C. & Stapp, M. Evidence for deformation associated with the 1998 eruption of Axial Volcano, Juan de Fuca Ridge, from acoustic extensometer measurements. *Geophys. Res. Lett.* **26**, 3441–3444 (1999).
7. Baker, E. T., Fox, C. G. & Cowen, J. P. In situ observations of the onset of hydrothermal discharge during the 1998 submarine eruption of Axial Volcano, Juan de Fuca Ridge. *Geophys. Res. Lett.* **26**, 3445–3448 (1999).
8. Griffiths, R. W. & Fink, J. H. Solidification and morphology of submarine lavas: A dependence on extrusion rate. *J. Geophys. Res.* **97**, 19729–19737 (1992).
9. Gregg, T. K. P. & Fink, J. H. Quantification of submarine lava-flow morphology through analog experiments. *Geology* **23**, 73–76 (1995).
10. Gregg, T. K. P. & Chadwick, W. W. Jr. Submarine lava-flow inflation: A model for the formation of lava pillars. *Geology* **24**, 981–984 (1996).
11. Chadwick, W. W. Jr, Gregg, T. K. P. & Embley, R. W. Submarine lineated sheet flows: A unique lava morphology formed on subsiding lava ponds. *Bull. Volcanol.* **61**, 194–206 (1999).
12. Fox, C. G. Evidence of active ground deformation on the mid-ocean ridge: Axial Seamount, Juan de Fuca Ridge, April–June, 1988. *J. Geophys. Res.* **95**, 12813–12822 (1990).
13. Gregg, T. K. P. & Fornari, D. J. Long submarine lava flows: Observations and results from numerical modeling. *J. Geophys. Res.* **103**, 27517–27532 (1998).
14. Wadge, G. The variation of magma discharge during basaltic eruptions. *J. Volcanol. Geotherm. Res.* **11**, 139–168 (1981).
15. Lockwood, J. P. & Lipman, P. W. Holocene eruptive history of Mauna Loa Volcano. *Prof. Pap. US Geol. Surv.* **1350**, 509–536 (1987).
16. Wolfe, E. W., Neal, C. A., Banks, N. G. & Duggan, T. J. Geologic observations and chronology of eruptive events. *Prof. Pap. US Geol. Surv.* **1463**, 1–98 (1988).
17. Rowland, S. K. & Walker, G. P. L. Pahoehoe and a'a in Hawaii: Volumetric flow rate controls the lava structure. *Bull. Volcanol.* **52**, 615–628 (1990).

18. Thordarson, T. & Self, S. The Laki (Skaftár Fires) and Grimsvötn eruptions in 1783–1785. *Bull. Volcanol.* **55**, 233–263 (1993).
19. Mogi, K. Relations between the eruptions of various volcanoes and the deformation of the ground surfaces around them. *Bull. Earthquake Res. Inst. Univ. Tokyo* **36**, 99–134 (1958).
20. West, M. E., Menke, W. & Tolstoy, M. Massive magma reservoir beneath Axial volcano, Juan de Fuca ridge. *Nature* (submitted).

Acknowledgements

We thank H. Milburn, C. Meinig and P. McLain for helping to build, maintain and rescue the VSM2 instrument; the ROPOS group and the crews of the NOAA ship *Ron Brown* and RV *Thompson* for their help with successful recovery of VSM2; and S. Carbotte and J. Fink for comments on the manuscript. This work was supported by the NOAA Vents Program and the West Coast and Polar Regions Undersea Research Center.

Correspondence and requests for materials should be addressed to W.W.C. (e-mail: chadwick@pmel.noaa.gov).

.....
Spanwise flow and the attachment of the leading-edge vortex on insect wings

James M. Birch & Michael H. Dickinson

Department of Integrative Biology, University of California, Berkeley, California 94720, USA

.....
 The flow structure that is largely responsible for the good performance of insect wings has recently been identified as a leading-edge vortex^{1,2}. But because such vortices become detached from a wing in two-dimensional flow¹, an unknown mechanism must keep them attached to (three-dimensional) flapping wings. The current explanation, analogous to a mechanism operating on delta-wing aircraft, is that spanwise flow through a spiral vortex drains energy from the vortex core³. We have tested this hypothesis by systematically mapping the flow generated by a dynamically scaled model insect while simultaneously measuring the resulting aerodynamic forces. Here we report that, at the Reynolds numbers matching the flows relevant for most insects, flapping wings do not generate a spiral vortex akin to that produced by delta-wing aircraft. We also find that limiting spanwise flow with fences and edge baffles does not cause detachment of the leading-edge vortex. The data support an alternative hypothesis—that downward flow induced by tip vortices limits the growth of the leading-edge vortex.

The failure of conventional theory to explain the hovering flight of insects prompted the search for unsteady aerodynamic mechanisms that could account for the good performance of flapping wings. One such mechanism, dynamic stall, is manifest by the formation of a leading-edge vortex (LEV) on the top surface of the wing at high angles of attack^{1–5}. However, in both experimental and computational studies of two-dimensional (2D) wings started from rest, the LEV builds in strength until it detaches from the wing and is shed into the wake, being replaced by a trailing-edge vortex of the opposite sign^{6,7}. This pattern of vortex growth and shedding repeats, giving rise to a trail of counter-rotating vortices known as a Kármán street. In three-dimensional (3D) models of both hawkmoths (*Manduca sexta*) and fruitflies (*Drosophila melanogaster*), the LEV is not quickly shed, but rather remains attached to the wing throughout the stroke^{3,8,9}. There are currently two hypotheses to explain this prolonged attachment of the LEV in 3D flows. One possibility, analogous to a mechanism thought to stabilize an attached vortex on delta-wing aircraft such as Concorde¹⁰, is that base-to-tip spanwise flow in the form of a spiral vortex limits the